Electronic Supplementary Material (ESI) for Chemical Communications.

Electronic supplementary information

Bismuth with abundant defects for electrocatalytic CO_2 reduction and Zn-CO_2 batteries

Chemicals:

All reagents were of analytical grade and used without further purification. The bismuth neodecanoate ($C_{30}H_{57}BiO_6$) was purchased from Aladdin Industrial Corporation. The polyvinylpyrrolidone (PVP) was purchased from Energy Chemical Co., Ltd. The ethylene glycol ($(CH_2OH)_2$), ascorbic acid ($C_6H_8O_6$), ethanol (C_2H_5OH), potassium bicarbonate ($KHCO_3$), potassium hydroxide (KOH) and dimethyl sulfoxide (DMSO) were purchased from Sinopharm Chemical Reagent Co., Ltd. The Nafion 211 membrane, anion membrane (FAB-PK-130), bipolar membrane (FBM-PK), carbon paper, gas diffusion layer, carbon rods and glassy carbon electrode were purchased from Gaoss Union Technology Co., Ltd. The commercial Bi powder with the size of 200 mesh was purchased from Macklin Biochemical Co., Ltd. The commercial Ir/C (10 wt%) catalyst was purchased from Shanghai Hesen Co., Ltd. The deuterated water (D_2O) was purchased from Saibole Technology Co., Ltd. All the deionized water (18.25 kΩ) used for solution preparation and instrument cleaning was homemade by UPT-II-10T ultrapure water system.

Synthesis:

To prepare Bi-D, $C_{30}H_{57}BiO_6$ was used as Bi precursor. $C_6H_8O_6$ was used as reducing agent. PVP was used as surfactant. And $(CH_2OH)_2$ was used as solvent. Briefly, 1 mmol $C_{30}H_{57}BiO_6$ and 300 mg PVP were first uniformly dispersed in 15 mL $(CH_2OH)_2$ to form a clear solution A. Then, 2 mmol $C_6H_8O_6$ was uniformly dispersed in 25 mL $(CH_2OH)_2$ to form a clear solution B. After mixing solution A and B thoroughly, transferring them into a 50 ml Teflon-lined autoclave and kept at 150°C for 4 hours in an oven. The prepared black precipitate was washed with ethanol and deionized water alternately for three times, which then dried in a vacuum oven at 60℃ to obtained Bi-D. For comparison, the Bi-D (2/2) and Bi-D (2/3) were also synthesized by adjusting the ratio of Bi precursor and reducing agent to 2: 2 and 2: 3 (mmol: mmol), respectively. Other synthesis conditions were the same as Bi-D.

Characterization:

The X-ray diffraction (XRD) patterns of catalysts were recorded on an X-ray diffractometer (D/max 2550) with Cu Kα radiation at a scan rate of 10° min^{-1} from 10° to 80°. The Raman spectra were tested by a Raman spectrometer (LabRAM HR apparatus) with a test range from 0 to 2000 cm^{-1}. For X-ray photoelectron spectroscopy (XPS), a Thermo Fisher Escalab 250Xi XPS instrument with Al Kα as emission source was applied. The spectra were calibrated with the position of C 1s

peak (284.8 eV). The FEI TECNAI G2 F20 transmission electron microscope (TEM) was used to observe the morphology of catalysts and analyze their internal structure.

Electrochemical measurements:

To prepare catalyst ink, 6 mg freshly prepared sample and 2 mg acetylene black were dispersed in 970 μl isopropanol/H_2O (1:3) solution containing 30 μL nafion membrane solution. After continuous ultrasound treatment for 2 h, 40 μL catalyst ink was uniformly dripped on a piece carbon paper in a 0.5 cm×0.5 cm area (catalyst loading of 0.96 mg cm^{-2}). After drying at 60℃, the carbon paper with catalysts was directly used as work electrode. Using an electrochemical workstation (CHI 660E), the electrochemical measurements were carried out in a H-type cell with the three-electrode system and Nafion 117 membrane as a separator. The Ag/AgCl electrode and carbon rod served as reference electrode and counter electrode, respectively. And the 0.5 M $KHCO_3$ aqueous solution (30 mL for each half cell) was used as electrolyte. Linear sweep voltammetry (LSV) curves were recorded at the scanning rate of 5 mV s^{-1} after the continuous Ar/CO_2 (99.99%) bubbling more than 30 min. For constant voltage electrolysis, the CO_2 delivered into cathodic electrolyte kept an average rate of 10 mL min^{-1} during the whole electrolysis process. All voltages were calibrated to potentials relative to reversible hydrogen electrode (RHE) according to the equation:

$$E_{RHE} = E_{Ag/AgCl} + 0.0591 \times pH + 0.197 \text{ V}.$$

The electrochemical active surface area (ECSA) was estimated from the electrochemical double-layer capacitance (C_{dl}). To eliminate the impact of carbon paper, the 15 μL prepared catalyst ink without acetylene black was coated on a smooth glassy carbon electrode (0.196 cm^2). In this case, a typically potential window of 0.1 V in non-Faradaic potential range was selected. With the scan rates of 20, 50, 80, 100 and 120 mV s^{-1}, the cyclic voltammetry curves were separately recorded in a single cell applying 0.5 M $KHCO_3$ as electrolyte. Using the Δj ($\Delta j = j_a - j_c$, j_c and j_a respectively represented the cathodic and anodic current densities under the OCP) against the scan rate to linearly fit a line, half of the slope was the value of C_{dl}. Assuming the average C_{dl} of metal was 20 μF cm^{-2}, it can be concluded as follows:

$$ECSA = S \times R_f = S \times C_{dl} / (20\ \mu F\ cm^{-2})$$

Here, the R_f was roughness factor; S was the surface area of catalytic electrode (0.196 cm^{-2}).

The electrochemical impedance spectroscopy (EIS) were evaluated in a similar electrochemical device of ECSA. The test voltage was set to -0.9 V, while the test frequency was

10^{-2}-10^{6} Hz.

For flow cell configurations, the gas diffusion layers loading Bi-D (1 mg cm^{-2}) and commercial Ir/C (1 mg cm^{-2}) served as cathode and anode catalysts, respectively. Both the catholyte and anolyte were 1 M KOH, which were separated by an anion membrane. The flow rate of CO_2 was 20 mL min^{-1}, while the flow rate of electrolyte was 10 mL min^{-1}. Other test conditions were similar to CO_2RR process in a H-type electrolyzer.

The Zn-CO_2 batteries applied flow cell configurations. The gas diffusion layer loading Bi-D and Zn plate served as battery electrodes. The 2 M $KHCO_3$ + 0.02 $HCOO^-$ and 2 M KOH + 0.02 M $Zn(AC)_2$ served as electrolytes, which were separated by a bipolar membrane. During the test, the flow rates of electrolyte and CO_2 were controlled to be 10 mL min^{-1} and 20 mL min^{-1}, respectively. The LSV curves were recorded at the scanning rate of 5 mV s^{-1}. The rate performance was evaluated by galvanostatic discharge at 1, 2 and 5 mA cm^{-2}. For charge/discharge cycle, the current density was set to 5 mA cm^{-2}, and the continuous discharge or charge time was 600 s.

Product analysis:

After electrolysis process, the gas products collected by air bags were detected through a gas chromatograph (GC) equipped with a thermal conductivity detector and a flame ionization detector, which could respectively quantify the H_2 and CO. The Ar (99.99%) acted as carrier gas. Before experiment, the GC was calibrated by standards gas (CO and H_2) with different concentrations. The liquid products were measured by nuclear magnetic resonance (NMR) spectroscopy (600 M). Typically, 0.3 mL electrolyte first mixed with 0.1 ml D_2O. Then, 50 μL dimethyl sulfoxide solution (40 μL DMSO diluted into 40 mL deionized water) was dropped as an internal standard.

The Faraday efficiency (FE) of different reduction products can be calculated as follows: $FE = c \times V \times n \times F \times Q^{-1}$

Here, c represented the concentration of products; V represented the total volume; n was the number of transferred electrons, which was 2 for both CO, H_2 and $HCOO^-$; F was the Faraday constant (96485 C mol^{-1}); Q was the total charge passing through the circuit during electrolysis, which can be recorded by electrochemical workstation. Further, the partial current density $j_p = j_{total} \times FE \times S^{-1}$.

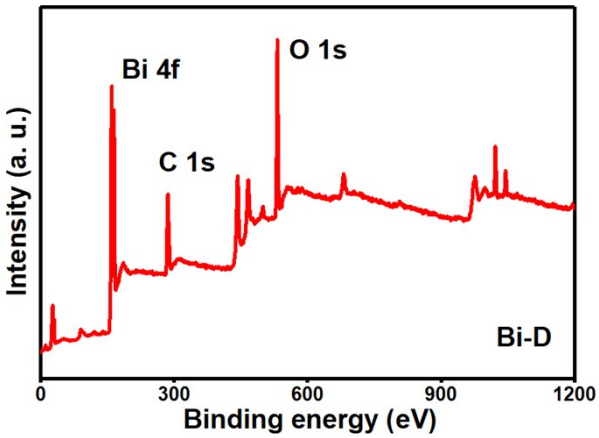

Fig. S1 The XPS survey of Bi-D.

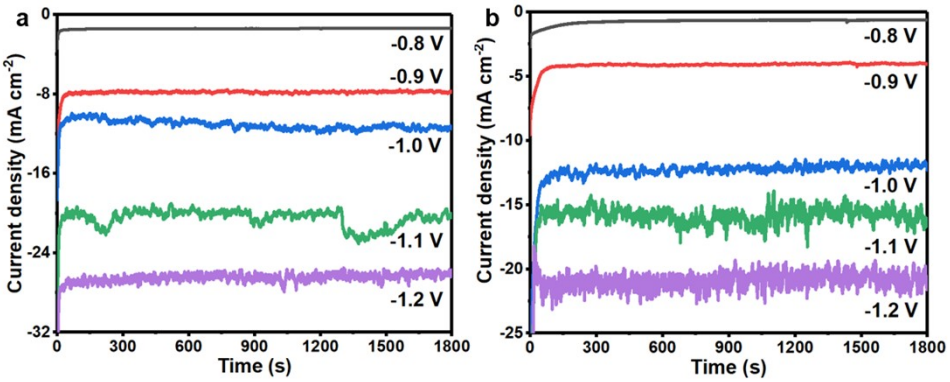

Fig. S2 The I-t curves of (a) Bi-D and (b) Bi-C.

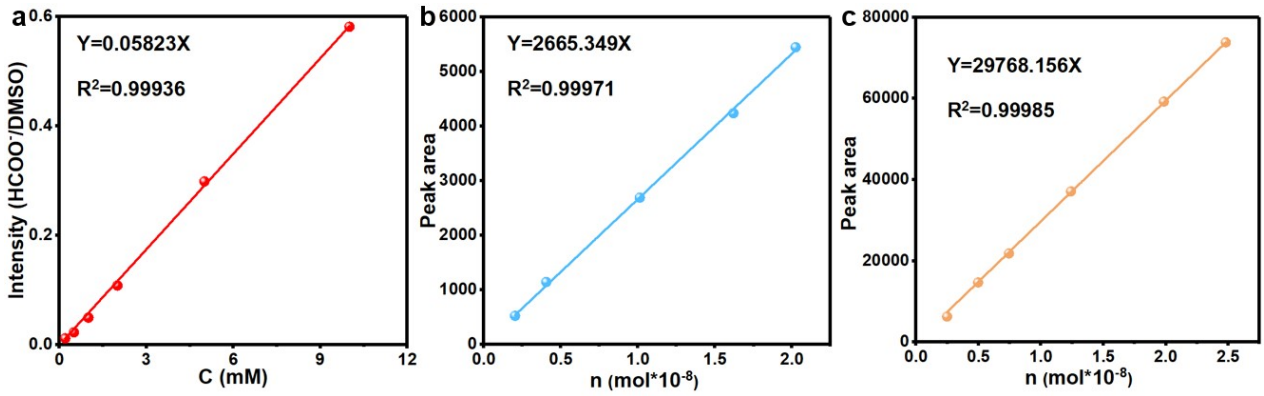

Fig. S3 The standard curves of (a) $HCOO^-$, (b) H_2 and (c) CO.

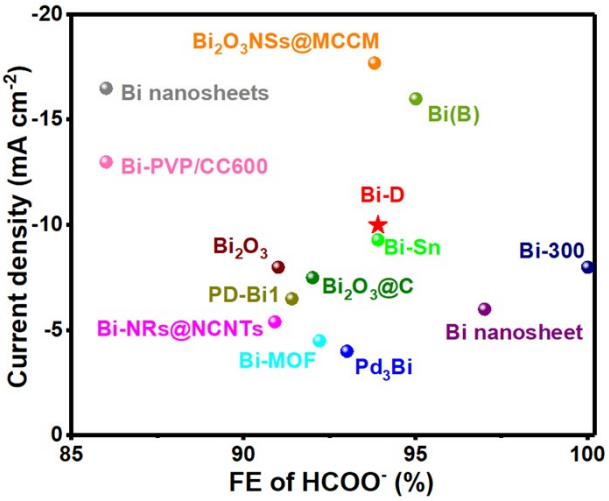

Fig. S4 The property comparison of partial Bi-based catalysts.

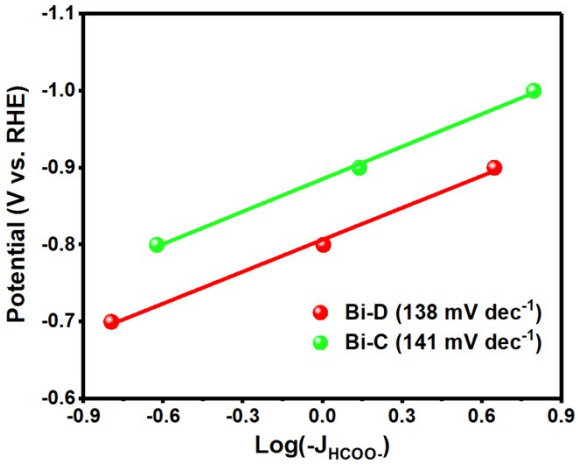

Fig. S5 The Tafel plots of Bi-D and Bi-C.

Bi-D and Bi-C exhibited close Tafel slopes, indicating that their rate-determining steps were both the first electron transfer.

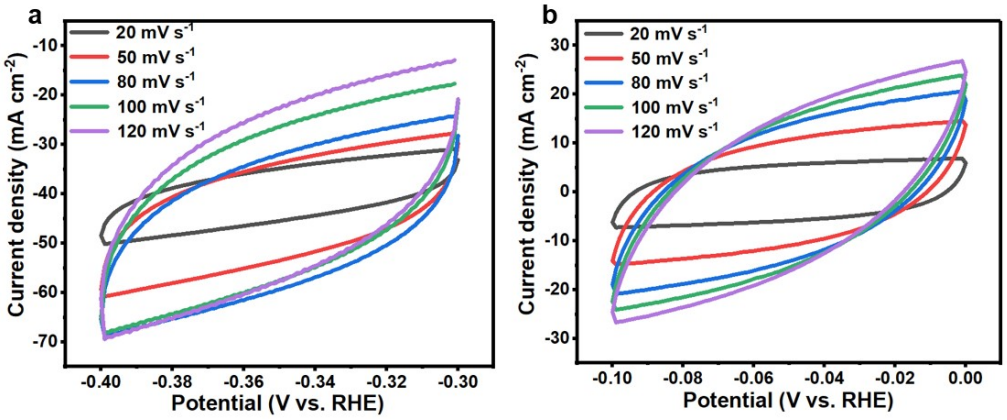

Fig. S6 The CV curves with different scan rates of (a) Bi-D and (b) Bi-C.

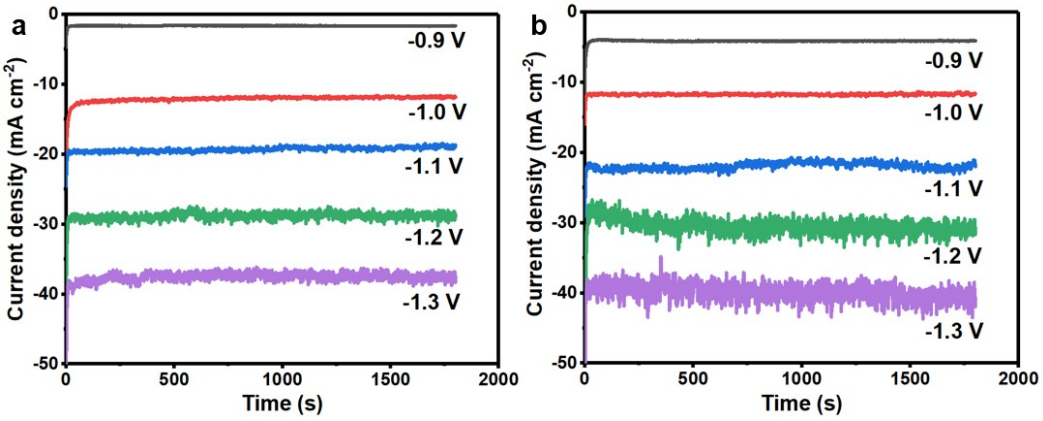

Fig. S7 The I-t curves of (a) Bi-D (2/2) and (b) Bi-D (2/3).

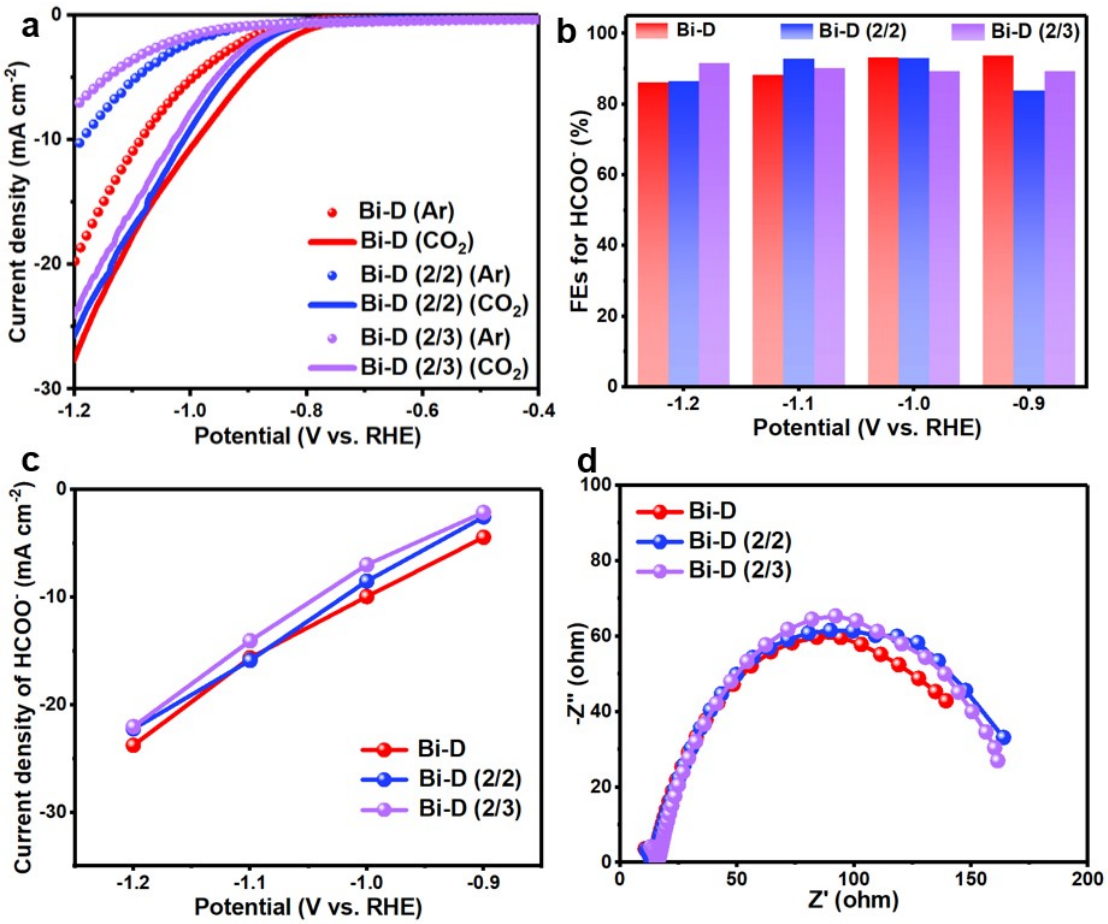

Fig. S8 (a) The LSV curves towards different samples under saturated Ar or CO_2 atmosphere. (b) The comparison of $HCOO^-$ FEs between different samples. (c) The comparison of $HCOO^-$ partial current densities towards different samples. (d) The EIS results of different samples.

The Bi-D (2/2) and Bi-D (2/3) (content of bismuth neodecanoate/content of ascorbic acid, mmol/mmol) were prepared. According to the results of electrolysis curves, it can be found that the current densities of Bi-D, Bi-D (2/2) and Bi-D (2/3) were similar. Correspondingly, their $HCOO^-$ selectivity, partial current densities and EIS results were also close. Thus, defects were important factors to achieve optimized CO_2RR performance. And such a preparation process for defect formation was adjustable.

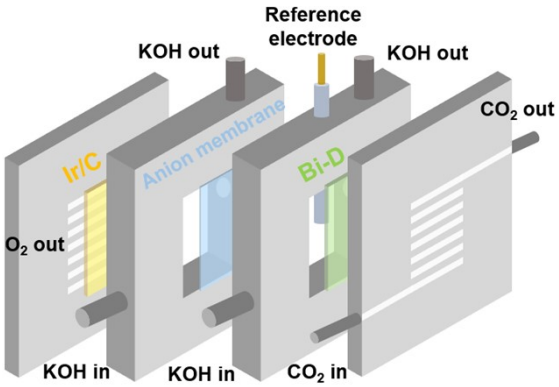

Fig. S9 The structure diagram of a flow cell.

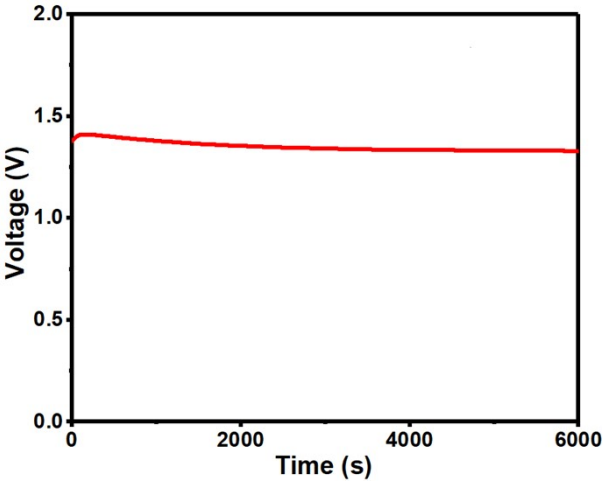

Fig. S10 The OCP test of Bi-D under saturated CO_2 atmosphere.

Table S1. The element contents of Bi-D from XPS results.

Elements	**Bi**	**C**	**O**	**N**
Content (at%)	4.81	54.45	38.41	2.33

Table S2. The property comparison towards Bi-based catalysts for electrocatalytic CO_2RR.

Catalyst	Electrolyte	FE (%)	J_{HCOO^-} (mA cm^{-2})	Reference
Bi-D	**0.5 M $KHCO_3$**	**93.9 (-0.9 V)**	**-10 (-1.0 V)**	**This work**
Bi-Sn	0.5 M $KHCO_3$	93.9 (-1.0 V)	-9.3 (-1.0 V)	Angew. Chem. Int. Ed. 2021, 60, 12554
Pd_3Bi	0.1 M $KHCO_3$	93 (-0.33 V)	-4 (-0.33 V)	Angew. Chem. Int. Ed. 2021, 60, 21741
Bi-MOF	0.1 M $KHCO_3$	92.2 (-0.9 V)	-4.5 (-0.9 V)	Appl. Catal. B-Environ. 2020, 277, 119241
PD-Bi1	0.5 M $KHCO_3$	91.4 (-0.9 V)	-6.5 (-0.9 V)	Angew. Chem. Int. Ed. 2021, 60, 7681
Bi-NRs@NCNTs	0.1 M $KHCO_3$	90.9 (-0.9 V)	-5.4 (-0.9 V)	Nano Lett. 2021, 21, 2650
Bi-300	0.5 M $KHCO_3$	~100 (-0.7 V)	-8 (-0.7 V)	Angew. Chem. Int. Ed. 2020, 59, 20112
Bi nanosheet	1 M $KHCO_3$	97 (-0.8 V)	-6 (-0.8 V)	Appl. Catal. B-Environ. 2020, 266, 118625
Bi_2O_3	0.5 M $KHCO_3$	91 (-0.9 V)	-8 (-0.9 V)	ACS Catal. 2020, 10, 743
f-Bi_2O_3	0.1 M $KHCO_3$	87 (-1.2 V)	-20.9 (-1.2 V)	Adv. Funct. Mater. 2020, 30, 1906478
Bi_2O_3@C	0.5 M $KHCO_3$	92 (-0.9 V)	-7.5 (-0.9 V)	Angew. Chem. Int. Ed. 2020, 59, 10807
Bi_2O_3NSs@MCCM	0.1 M $KHCO_3$	93.8 (1.26 V)	-17.7 (-1.36 V)	Angew. Chem. Int. Ed. 2019, 58, 13828
D-CeOx/Bi	0.5 M $KHCO_3$	92 (-0.9 V)	-22 (-0.9 V)	Natl. Sci. Rev. 2021, 8, nwaa187
Bi-PVP/CC600	0.5 M $KHCO_3$	86 (-0.83 V)	-13 (-0.83 V)	Appl. Catal. B-Environ. 2021, 284, 119723
Bi nanosheets	0.5 M $KHCO_3$	86 (-1.1 V)	-16.5 (-1.1 V)	Nano Energy 2018, 53, 808
Bi(B)	0.5 M $KHCO_3$	95 (-0.9 V)	-16 (-0.9 V)	Small 2021, 2101128